HIGHLIGHTED ARTICLE
GENETICS | INVESTIGATION

The Relative Contributions of the *X* Chromosome and Autosomes to Local Adaptation

Clémentine Lasne, Carla M. Sgrò, and Tim Connallon[1]
School of Biological Sciences, Monash University, Clayton 3800, Australia

ABSTRACT Models of sex chromosome and autosome evolution yield key predictions about the genomic basis of adaptive divergence, and such models have been important in guiding empirical research in comparative genomics and studies of speciation. In addition to the adaptive differentiation that occurs between species over time, selection also favors genetic divergence across geographic space, with subpopulations of single species evolving conspicuous differences in traits involved in adaptation to local environmental conditions. The potential contribution of sex chromosomes (the *X* or *Z*) to local adaptation remains unclear, as we currently lack theory that directly links spatial variation in selection to local adaptation of *X*-linked and autosomal genes. Here, we develop population genetic models that explicitly consider the effects of genetic dominance, effective population size, and sex-specific migration and selection on the relative contributions of *X*-linked and autosomal genes to local adaptation. We show that *X*-linked genes should nearly always disproportionately contribute to local adaptation in the presence of gene flow. We also show that considerations of dominance and effective population size—which play pivotal roles in the theory of faster-*X* adaptation between species—have surprisingly little influence on the relative contribution of the *X* chromosome to local adaptation. Instead, sex-biased migration is the primary mediator of the strength of spatial large-*X* effects. Our results yield novel predictions about the role of sex chromosomes in local adaptation. We outline empirical approaches in evolutionary quantitative genetics and genomics that could build upon this new theory.

KEYWORDS cline; adaptation; sex linkage; dominance; effective population size

THEORETICAL models of adaptation have expanded dramatically during the last two decades, and have taken central roles in defining many of the core conceptual questions that currently drive empirical research in evolutionary genetics and genomics. What is the distribution of phenotypic effects among beneficial mutations and fixed genetic variants (*e.g.*, Orr 1998, 2006; Martin and Lenormand 2008)? What is the relative importance of new mutations *vs.* standing genetic variation during the process of adaptation (*e.g.*, Hill 1982; Orr and Betancourt 2001; Hermisson and Pennings 2005)? What evolutionary rules, if any, govern the dynamics of adaptation in DNA sequence space (Smith 1970; Gillespie 1991; Orr 2002)? How do population genetic parameters like effective population size and the fitness effects of new mutations influence genome-wide patterns of adaptive genetic divergence among species (Gillespie 2004; McCandlish and Stoltzfus 2014), and between different regions of a genome (Charlesworth 1992; Orr 2010; Glémin and Ronfort 2013)? These theories have also been instrumental for interpreting a wide array of empirical patterns, ranging from microbial experimental evolution (Martin and Lenormand 2006) to genetic dissections of quantitative traits (Orr 2005).

Faster-*X* theory has been particularly useful in driving empirical research on the evolutionary genetics of adaptation (Meisel and Connallon 2013) and the genetics of reproductive isolation between species (Presgraves 2008). This theory focuses on the relative rates of evolution on sex chromosomes and autosomes, and the population genetic conditions that lead to a differential accumulation of adaptive substitutions at sex-linked relative to autosomal loci. We now know of several factors that can influence the relative rates of *X vs.* autosome substitution, including the genetic dominance of beneficial mutations (Charlesworth *et al.* 1987), sex differences in selection (Charlesworth *et al.* 1987), sex-biased mutation rates (Kirkpatrick and Hall 2004; Vicoso and Charlesworth 2009), mechanisms of dosage compensation

doi: 10.1534/genetics.116.194670
Manuscript received August 8, 2016; accepted for publication December 25, 2016; published Early Online January 4, 2017.
Supplemental material is available online at www.genetics.org/lookup/suppl/doi:10.1534/genetics.116.194670/-/DC1.
[1]Corresponding author: School of Biological Sciences, Monash University, Bldg. 18, Clayton, VIC 3800, Australia. E-mail: tim.connallon@monash.edu

(Charlesworth *et al.* 1987; Vicoso and Charlesworth 2009), adaptation from new mutations *vs.* standing genetic variation (Orr and Betancourt 2001; Connallon *et al.* 2012), distinct effective population sizes of different chromosomes (Vicoso and Charlesworth 2009), and epistasis (Connallon *et al.* 2012). Faster-*X* research has particularly emphasized the interplay between genetic dominance and adaptation (*e.g.*, Orr 2010; Meisel and Connallon 2013). Theory predicts that *X*-linked genes should adapt more rapidly than the autosomes when beneficial mutations are partially or completely recessive. Consequently, the frequent empirical observations of faster-*X* rates of adaptive substitution could imply that beneficial alleles are, on average, partially recessive (for discussion, see Presgraves 2008; Mank *et al.* 2010; Orr 2010; Meisel and Connallon 2013). The faster-*X* theory may also explain the disproportionately large contribution of *X*-linked genes to reproductive incompatibility between species (Coyne and Orr 1989; Masly and Presgraves 2007).

Faster-*X* theory has largely focused on long-term patterns of evolutionary change and their implications for adaptive differentiation between species. In contrast, this theory is largely silent regarding the role of the *X* chromosome in adaptive differentiation between subpopulations of single species, in response to local environmental conditions (for exceptions, see: Owen 1986; Nagylaki 1996; Parker and Hedrick 2000). The balance between migration and spatially variable selection has been a major focus of classical population genetics theory, which includes the maintenance of genetic differences between populations exchanging migrants (Moran 1959, 1962), the theory of clines (Haldane 1948; Fisher 1950), and the maintenance of genetic polymorphism in spatially complex environments (Levene 1953; Felsenstein 1976; Hedrick *et al.* 1976; Hedrick 1986, 2006). Recent theory has expanded upon this classical framework by considering, for example, the evolutionary genetic basis of convergent adaptation among subpopulations of geographically widespread species (Ralph and Coop 2010), and the population genetics of adaptation at species' range margins (Peischl *et al.* 2013, 2015). However, despite widespread interest in the genetics of adaptation across geographic space (Hoban *et al.* 2016), the potential contributions of *X*-linked and autosomal genes to local adaptation have been largely overlooked. Theoretically, we have little to guide predictions about the relative contributions of the *X* and autosomes to local adaptation.

Here, we address this gap in theory by merging classical population genetic models of local adaptation (*e.g.*, Haldane 1948; Moran 1959, 1962) and *X*-chromosome evolution (*e.g.*, Haldane 1924; Avery 1984). We specifically investigate the relative contributions of *X*-linked and autosomal loci to local adaptation across abrupt and continuous environmental gradients (results can also be applied to *Z*-linkage in species with female-heterogametic sex determination, *e.g.*, birds and Lepidoptera). Our models jointly consider the effects of sex-biased migration, sex differences in selection, genetic dominance, and the effective population sizes of *X*-linked and autosomal loci on the extent of spatial adaptive differentiation at *X*-linked and autosomal loci. In contrast to the theory of faster-*X* divergence between species—where dominance plays a major role in shaping the relative rates of *X vs.* autosome substitution—we find that the relative contribution of the *X* to local adaptation is largely determined by sex-specific migration rates and is relatively insensitive to the dominance coefficients of locally adapted alleles. The models predict a "spatial large-*X* effect" over most of the parameter space of dominance and sex-specific selection, particularly when migration rates are male biased.

Model

In contrasting the responses of autosomal and *X*-linked loci to selection for local adaptation, we take three complementary approaches. First, we built upon Moran's influential model of divergence between a pair of differentially selected populations (Moran 1959, 1962; Charlesworth and Charlesworth 2010, Chapter 4; Felsenstein 2015) to quantify equilibrium genetic divergence under migration-selection balance. Second, we extended classical cline theory (Haldane 1948; Charlesworth and Charlesworth 2010, Chapter 4; Felsenstein 2015) to develop analytical predictions for the slopes of *X*-linked and autosomal clines. Third, we carried out stochastic forward simulations of genetic clines under migration, selection, and genetic drift in a one-dimensional stepping-stone model with discrete habitats distributed along an environmental gradient. For each model, we follow the frequencies of two alleles per locus. We arbitrarily label the alleles *A* and *B*, with q referring to the frequency of allele *A*, and $1 - q$ to the frequency of *B*. Each allele is favored in the different populations, or in different locations across the environmental gradient.

Moran's two-population model

Following Moran (1959, 1962), we considered a symmetrical, two-population model in which the *A* allele is favored in one of the populations and the *B* allele is favored in the other (see Table 1 for the sex-specific fitness parameterization for each population and mode of inheritance). Effects of drift are assumed to be negligible. We also assume three forms of symmetry in the model: (1) equal migration rates between populations 1 and 2, (2) equal selection coefficients against the inferior homozygote genotype within each population, and (3) equal population sizes.

As in earlier work (*i.e.*, using autosomal models; see Charlesworth and Charlesworth 2010, Chapter 4) we assume that the rate of migration (d) and strength of selection (s) are both weak (d and s are both small), and we can therefore approximate the total rate of change in allele frequencies, per population, as the sum of the expected changes under migration and selection, individually. Specifically, we model the total change in frequency of an arbitrary, focal population as:

$$\Delta q = \Delta q_{\text{mig}} + \Delta q_{\text{sel}}, \tag{1a}$$

where Δq_{mig} and Δq_{sel} represent the net change in frequency within the focal population due to migration and to local

Table 1 Fitness values by genotype, sex, and location for the abrupt environmental change model

Sex	Moran model	Cline model	Fitness value per genotypes		
			AA, *A*	*AB*	*BB*, *B*
Female	Pop. 1	$x < 0$	$1 - s_f$	$1 - s_f h_1$	1
	Pop. 2	$x > 0$	1	$1 - s_f h_2$	$1 - s_f$
Male (autosome)	Pop. 1	$x < 0$	$1 - s_m$	$1 - s_m h_1$	1
	Pop. 2	$x > 0$	1	$1 - s_m h_2$	$1 - s_m$
Male (*X*-linked)	Pop. 1	$x < 0$	$1 - s_m$	—	1
	Pop. 2	$x > 0$	1	—	$1 - s_m$

Pop., population.

selection, respectively. Expressions for Δq_{sel} are presented further below. Change in population 1 due to migration is given by $\Delta q_{mig} = (q_2 - q_1)d$, where q_1 and q_2 represent the frequencies of A in population 1 and 2, respectively, and d refers to the fraction of gene copies that migrate between the populations. The frequency change in population 2 due to migration is $\Delta q_{mig} = (q_1 - q_2)d$. Following prior theory (Berg *et al.* 1998; Laporte and Charlesworth 2002; Hedrick 2007), the migration rate for an autosomal locus is $d_A = (d_f + d_m)/2$; the migration rate for an *X*-linked locus is $d_X = (2d_f + d_m)/3$. Note that d is roughly analogous to the migration parameter, m, that we use in the subsequent cline models. We distinguish between m and d to avoid confusion about the slightly different definitions of migration in Moran and cline models of local adaptation.

Cline model

In our cline model, the population is spread with uniform density across a continuous, one-dimensional environmental gradient (with location represented by x). Migration is symmetrical in direction, and the strengths of migration and selection are assumed to be weak. Effects of drift are assumed to be negligible. Under these conditions, the equilibrium reaction-diffusion equation describing allele frequency at location x is:

$$\frac{m}{2}\frac{d^2q}{dx^2} + \Delta q_{sel} = 0, \tag{1b}$$

where m refers to the mean-squared dispersal distance of individuals relative to their locations at birth (incidentally, this parameter is functionally equivalent to the migration rate between adjacent habitats in a stepping-stone model; see Felsenstein 2015), and Δq_{sel} is the local response to selection, in terms of the change in frequency of the A allele. The migration parameter m takes into account differential migration rates between the sexes. Similar to the two-population model from above, the net migration rate for an autosomal locus is $m_A = (m_f + m_m)/2$, where m_f and m_m are female and male migration rates, respectively, and the net migration rate for an *X*-linked locus is $m_X = (2m_f + m_m)/3$.

We assume that the environment changes abruptly at location $x = 0$ along the gradient (*i.e.*, this model involves a step cline; Haldane 1948). Allele B is favored in one direction away from the environmental transition (when $x < 0$), while A is favored in the other direction ($x > 0$). In the step-cline model, the strength of selection for or against the A allele switches abruptly at the environmental transition, but then remains constant further away from the transition point (see Figure 1, left and middle panels, and Table 1). We characterize selection in each sex relative to the fittest genotype, with sex-specific selection coefficients (s_f, s_m) representing the strength of selection against the least-fit genotype, per location.

Genetic dominance and local responses to selection

Parameters h_1 and h_2 represent the dominance coefficients for locally maladaptive alleles (Table 1): h_1 refers to the relative dominance of the A allele in population 1 (in the Moran model) and in regions where $x < 0$ (in the cline model); h_2 refers to the dominance of B in population 2 (Moran) and in regions where $x > 0$ (cline model). Alleles have codominant, or "additive," fitness effects when $h_1 = h_2 = 1/2$. Following the previous theory on opposing selection between environments (see Curtsinger *et al.* 1994; Prout 2000; Fry 2010), we consider two idealized models of allelic dominance across the species' range. First, we consider a "beneficial reversal of dominance" model (hereafter "dominance reversal"; see Curtsinger *et al.* 1994), where $h = h_1 = h_2 < 1/2$. In this instance, allele A is dominant to B in locations where A is favored, and allele B is dominant to A in locations where B is favored (see Figure 1, middle and right panels, and Table 1). This particular parameterization emerges in scenarios where fitness landscapes are concave around local fitness optima (see Fry 2010; Manna *et al.* 2011; Martin and Lenormand 2015). Second, we consider a model of "parallel dominance" (Curtsinger *et al.* 1994; also see Kidwell *et al.* 1977), where $h = h_1 = 1 - h_2$; h refers to the dominance of A relative to B (*i.e.*, A is recessive when $h < 1/2$, whereas A is dominant when $h > 1/2$; Figure 1, left panel). In this case, the dominance relation between A and B is constant across the entire species' range—a scenario that applies when there is a monotonic relation between location in the species' range and selection on a phenotype for which alleles exhibit consistent levels of dominance (*e.g.*, the melanism phenotype, with different populations favoring/disfavoring melanic forms).

Under weak, sex-specific selection ($0 < s_m, s_f \ll 1$), and beneficial reversal of dominance ($h = h_1 = h_2$), the change in frequency of the A allele at an autosomal locus can be described by the following equations. In regions of the species range where allele A is favored (population 2 of the Moran

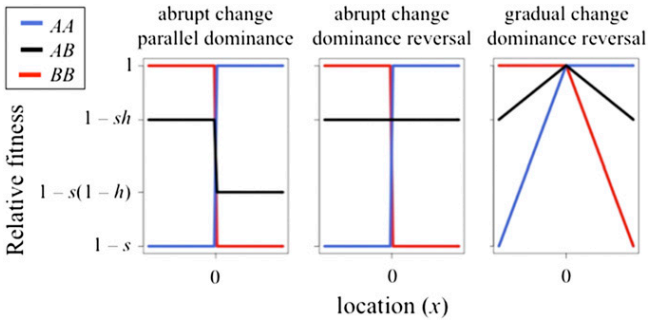

Figure 1 Spatial variation in relative fitness for each of the three genotypes (*AA*, *BB*, and *AB*). Examples of the dominance reversal scenario ($h = h_1 = h_2 = 0.3$; see Table 1) are shown in the center and right panels. An example of parallel dominance [$h = h_1 = (1 - h_2) = 0.3$; see Table 1] is shown in the left panel. Two scenarios of environmental change in fitness are shown: the first two panels depict a step cline in fitness that abruptly transitions at the center of the range (location $x = 0$); the third panel shows a ramp cline, with a gradual increase in the strength of selection away from the center of the range. Analytical results describe evolution under the abrupt change model and for each form of dominance (the first two panels). Simulations characterize evolution under all four scenarios of selection and dominance: the three scenarios depicted in the three panels, above, as well as the gradual change scenario with a dominance reversal (not depicted in figure).

model; $x > 0$ in the cline model), the local response to selection is given by:

$$\Delta q_{\text{sel}} = \frac{\Delta q_{\text{f}} + \Delta q_{\text{m}}}{2} \approx \frac{(s_{\text{f}} + s_{\text{m}})q(1-q)\left[1 - h - q(1-2h)\right]}{2}. \tag{2a}$$

Otherwise (Moran population 1; cline location $x < 0$), the local response to selection is:

$$\Delta q_{\text{sel}} = \frac{\Delta q_{\text{f}} + \Delta q_{\text{m}}}{2} \approx -\frac{(s_{\text{f}} + s_{\text{m}})q(1-q)\left[h + q(1-2h)\right]}{2}. \tag{2b}$$

For each expression, Δq_{f} and Δq_{m} refer to the frequency changes due to selection in females and males, respectively; the total frequency due to local selection is simply the average of sex-specific changes. For the *X* chromosome, local responses to selection are described by:

$$\Delta q_{\text{sel}} = \frac{2\Delta q_{\text{f}} + \Delta q_{\text{m}}}{3} \approx q(1-q)\frac{2s_{\text{f}}\left[1 - h - q(1-2h)\right] + s_{\text{m}}}{3} \tag{3a}$$

for population 2 or $x > 0$, and:

$$\Delta q_{\text{sel}} = \frac{2\Delta q_{\text{f}} + \Delta q_{\text{m}}}{3} \approx -q(1-q)\frac{2s_{\text{f}}\left[h + q(1-2h)\right] + s_{\text{m}}}{3} \tag{3b}$$

for population 1 or $x < 0$. The factor of two in $2\Delta q_{\text{f}}$ reflects the twofold higher rate of *X* chromosome transmission through mothers compared to fathers.

Under the parallel dominance scenario ($h = h_1 = 1 - h_2$), the local response to selection remains the same in population 1 and $x < 0$. For population 2 and $x > 0$, the response to selection on an autosome and *X*, respectively, is:

$$\Delta q_{\text{sel}} = \frac{\Delta q_{\text{f}} + \Delta q_{\text{m}}}{2} \approx \frac{(s_{\text{f}} + s_{\text{m}})q(1-q)\left[h + q(1-2h)\right]}{2} \tag{4a}$$

and:

$$\Delta q_{\text{sel}} = \frac{2\Delta q_{\text{f}} + \Delta q_{\text{m}}}{3} \approx q(1-q)\frac{2s_{\text{f}}\left[h + q(1-2h)\right] + s_{\text{m}}}{3}. \tag{4b}$$

Analysis of the models

We quantified equilibrium patterns of allele frequency differentiation among populations by analyzing Equation 1, a and b, using relevant expressions for *m*, *d* and Δq_{sel} for each model and mode of inheritance. Details of the Moran model analysis are presented in Appendix A. Details of the cline model analysis, which follows the approach outlined in Felsenstein (2015), are presented in Appendix B.

Moran model analysis: For the Moran model, we focused on two classes of results. First, assuming additive fitness effects ($h_1 = h_2 = 1/2$), the equilibrium frequency of *A* across the populations is $\hat{q} = (\hat{q}_1 + \hat{q}_2)/2 = 1/2$. For an autosomal locus, the allele frequency difference between populations is:

$$\delta_A = \hat{q}_2 - \hat{q}_1 = \sqrt{1 + \left[\frac{4(d_{\text{m}} + d_{\text{f}})}{s_{\text{m}} + s_{\text{f}}}\right]^2} - \frac{4(d_{\text{m}} + d_{\text{f}})}{s_{\text{m}} + s_{\text{f}}}. \tag{5a}$$

For an *X*-linked locus, the allele frequency difference between populations is:

$$\delta_X = \hat{q}_2 - \hat{q}_1 = \sqrt{1 + \left[\frac{2(2d_{\text{f}} + d_{\text{m}})}{s_{\text{m}} + s_{\text{f}}}\right]^2} - \frac{2(2d_{\text{f}} + d_{\text{m}})}{s_{\text{m}} + s_{\text{f}}}. \tag{5b}$$

Second, for cases where fitness effects are nonadditive, we obtained approximations for equilibrium allele frequencies, assuming that migration is high relative to selection (*e.g.*, $d \gg s$). For the dominance reversal model ($h = h_1 = h_2$), the overall allele frequency for each locus remains at $\hat{q} = (\hat{q}_1 + \hat{q}_2)/2 = 1/2$. The allele frequency difference between populations is well approximated (in the limit of high migration relative to selection) by:

$$\delta_A = \hat{q}_2 - \hat{q}_1 \approx \frac{s_{\text{m}} + s_{\text{f}}}{8(d_{\text{f}} + d_{\text{m}})}, \tag{6a}$$

for an autosomal locus, and

$$\delta_X = \hat{q}_2 - \hat{q}_1 \approx \frac{s_m + s_f}{4(2d_f + d_m)}. \quad (6b)$$

for an *X*-linked locus.

Under parallel dominance and autosomal linkage (and again, assuming $d \gg s$), the equilibrium frequency of *A* is:

$$\hat{q}_A = \frac{(1-3h) + \sqrt{1-3h(1-h)}}{3(1-2h)}, \quad (7a)$$

and the frequency differentiation between populations is:

$$\delta_A \approx \frac{\hat{q}_A(1-\hat{q}_A)\left[h + \hat{q}_A(1-2h)\right](s_m + s_f)}{d_m + d_f}. \quad (7b)$$

With parallel dominance and *X*-linkage, we get:

$$\hat{q}_X = \frac{[2s_f(1-3h) - s_m] + \sqrt{[2s_f(1-3h) - s_m]^2 + 6(2s_f h + s_m)s_f(1-2h)}}{6s_f(1-2h)}, \quad (7c)$$

and

$$\delta_X \approx \frac{\hat{q}_X(1-\hat{q}_X)\left[2s_f(h + \hat{q}_X(1-2h)) + s_m\right]}{d_m + 2d_f}. \quad (7d)$$

Cline model analysis: For the cline model, approximations are based on the assumption that range boundaries are sufficiently far from the environmental transition point (at $x = 0$) that *A* eventually approaches fixation on one side of the transition point ($q \to 1$ as $x \to \infty$), and *B* approaches fixation on the other side ($q \to 0$ as $x \to -\infty$). Validity of this assumption does not necessarily require the species' range to be infinite; rather, selection must be sufficiently strong relative to the distance to each range boundary.

Under dominance reversal conditions, the autosome and *X*-linked cline maxima (respectively) are:

$$y_A = \sqrt{\frac{(5+6h)(s_f + s_m)}{48(m_f + m_m)}} \quad (8a)$$

and:

$$y_X = \sqrt{\frac{s_f(5+6h) + 8s_m}{24(2m_f + m_m)}}. \quad (8b)$$

In both cases, the equilibrium allele frequency at the corresponding midpoint of the species range is $\hat{q}_{x=0} = 0.5$.

Under parallel dominance, the cline maxima for autosomal and *X*-linked loci, respectively, are:

$$y_A = \sqrt{\frac{s_f + s_m}{6(m_f + m_m)}} \quad (9a)$$

and

$$y_X = \sqrt{\frac{s_f + s_m}{3(2m_f + m_m)}}. \quad (9b)$$

The equilibrium allele frequencies at the range center (under autosomal and *X*-linked inheritance, respectively) are:

$$\hat{q}_{A,\,x=0} \approx \frac{1}{2} + \frac{1-2h}{8} \quad (10a)$$

and

$$\hat{q}_{X,\,x=0} \approx \frac{1}{2} + \frac{s_f(1-2h)}{8(s_f + s_m)}. \quad (10b)$$

Simulations of the stepping-stone model

We expanded upon the analytical results by implementing a one-dimensional stepping-stone model that includes *H* discrete habitat patches (or "demes") (we assume *H* is an even integer), and discrete generations. Population size is constant over time and uniform across the demes. As before, we follow the frequencies of alleles *A* and *B* per locus.

We considered two patterns of selection across the environmental gradient. To facilitate comparisons with the analytical results, we first considered the case where fitness values per genotype shift abruptly at the range center (*i.e.*, between deme $H/2$ and deme $1 + H/2$). In this step-cline scenario, the *A* allele is favored in demes $1 + H/2$ through *H*, and the *B* allele is favored in demes 1 through $H/2$. The relative fitnesses of the three possible genotypes are equivalent to those depicted in Table 1. Second, we considered a model of gradually changing selection across demes. Selection again favors the *B* allele in demes 1 through $H/2$; *A* is favored in the remaining demes. The strength of selection for *A* or *B* increases away from the midpoint of the species range, and eventually reaches a maximum at the endpoints of the environmental gradient (see Figure 1 and Table 2). We considered the same forms of dominance as in the analytical models (*i.e.*, dominance reversal and parallel dominance).

The life cycle of the species follows the order of birth, migration, local selection within demes, and random mating among the adults of each deme (*i.e.*, after selection). For an arbitrary deme *i* between $i = 2$ and $i = H - 1$, each female and male has a probability m_f and m_m, respectively, of migrating to an adjacent deme, and a probability of $1 - m_f$ and $1 - m_m$ of remaining in the deme of birth. Migrating individuals are equally likely to migrate to each of the two adjacent demes (*i.e.*, individuals migrating from the *i*th deme are equally likely to land in deme $i - 1$ or in deme $i + 1$). Demes at the edge of the species range (demes 1 and *H*) exchange migrants with one neighboring deme. We assume that range boundaries are "reflecting" (see *e.g.*, Garcia-Ramos and Kirkpatrick 1997), with each female and male from deme 1 or deme *H* migrating to the adjacent deme (deme 2 or deme $H - 1$) with probabilities $m_f/2$ and $m_m/2$, respectively. Female and male individuals that are born in deme 1 or deme *H* remain with probability $1 - m_f/2$ and $1 - m_m/2$. We also

Table 2 Fitness values by genotype, sex, and location for the gradual environmental change model

Sex	Location	Fitness value per genotypes		
		AA, *A*	*AB*	*BB*, *B*
Female	$i \leq H/2$	$1 + s(i, \text{f})$	$1 + h_1 s(i, \text{f})$	1
	$i > H/2$	1	$1 - h_2 s(i, \text{f})$	$1 - s(i, \text{f})$
Male (autosome)	$i \leq H/2$	$1 + s(i, \text{m})$	$1 + h_1 s(i, \text{m})$	1
	$i > H/2$	1	$1 - h_2 s(i, \text{m})$	$1 - s(i, \text{m})$
Male (*X*-linked)	$i \leq H/2$	$1 + s(i, \text{m})$	—	1
	$i > H/2$	1	—	$1 - s(i, \text{m})$

The above applies in a stepping-stone model with H demes, where H is an even integer, s_j is a constant that represents the selection for the jth sex at each of the boundary demes, and $s(i, j)$ is a function representing the selection coefficient for the jth sex in the ith deme: $s(i, j) = s_j[2i - (1 + H)]/(H - 1)$.

considered a model where local selection occurs before migration and random mating, and found similar results. For simplicity, we present the results and recursions for models where migration occurs before selection (see Supplemental Material, File S1, for further details).

For point of comparison with the analytical results, we first carried out deterministic simulations for the abrupt and gradual environmental change models. Each simulation run was initiated with equal frequencies of the two alleles in each deme. Deterministic simulations were iterated for a minimum of 10,000 generations, which was sufficient to reach equilibrium. Cline slopes were calculated as the allele frequency difference between a given pair of adjacent demes. This approach to quantifying cline slope yields comparable results to the analytical cline model when allele frequency change is roughly linear across the species' range center; otherwise, estimates of the maximum cline slope are downwardly biased in the stepping-stone model (for discussion, see Chapter 4 of Felsenstein 2015). To ease comparison, we focused on parameter space leading to linear change near the center of the species' range (as when $s/m < 1$).

Genetic drift was incorporated by way of multinomial sampling of adult genotypes (see, *e.g.*, Charlesworth and Charlesworth 2010, pp. 229–230). We assumed that each deme produces N_f and N_m adult females and males that randomly mate (within demes) to produce offspring of the next generation. Following the standard Wright–Fisher model of drift (Charlesworth and Charlesworth 2010), we sampled genotypes for N_m males and N_f females from a multinomial distribution, with probabilities of each genotype based on the expected (deterministic) genotype frequencies for adults of the deme. Genotype frequencies of breeding adults (after sampling) were then used to calculate expected frequencies of adult genotypes in the next generation.

Assuming that individuals of each sex produce a Poisson-distributed number of offspring in each generation, then the autosomal and *X*-linked effective population sizes are simple functions of N_f and N_m (see Avery 1984; Hartl and Clark 2007, p. 124). The effective population size for an autosomal locus is $N_{eA} = 4N_\text{f}N_\text{m}/(N_\text{f} + N_\text{m})$, and the effective size for an *X*-linked locus is $N_{eX} = 9N_\text{f}N_\text{m}/(4N_\text{m} + 2N_\text{f})$. We note that there are more complex models for *X*-linked and autosome effective sizes that take into account different forms of reproductive success variance among breeding males and females (see Laporte and Charlesworth 2002; Vicoso and Charlesworth 2009). Our approach represents the simplest route to incorporate drift and different relative effective sizes of *X*-linked and autosomal genes. We specifically considered the effect of three different ratios of *X*-to-autosome effective population sizes on the evolution of cline slopes: (1) the null *X*/autosome ratio of $N_{eX}/N_{eA} = 0.75$, (2) a dampened *X*/autosome ratio of $N_{eX}/N_{eA} = 0.6$, and (3) an elevated *X*/autosome ratio of $N_{eX}/N_{eA} = 1$. For each set of selection, migration, and effective population size parameters we carried out 1000 replicate simulation runs. Each run was carried out for $2N_{eA}$ generations to eliminate effects of initial allele frequency conditions. All simulations were carried out in R version 3.1.2 (R Core Team 2014). A full description of the simulation algorithm can be found in File S1; corresponding R code has been deposited in GitHub (https://gist.github.com/ClemLasne).

Data availability

The authors state that all data necessary for confirming the conclusions presented in the article are represented fully within the article.

Results

In the following results, we focus on the amount of genetic divergence at *X*-linked relative to autosomal loci when each evolves in response to spatially varying selection. First, we present results for a two-population model of migration-selection balance (as in Moran 1959, 1962; Charlesworth and Charlesworth 2010, Chapter 4). Second, we present analytical results for allele frequency clines in a species that is continuously distributed across an abrupt environmental transition. Third, we present simulation results from a stepping-stone model of population subdivision, which expand upon the analytical predictions by considering both gradual *and* abrupt change in selection across space and genetic drift. Fourth, we quantify the relative contributions of the *X* and autosomes to the fitness load of migrant relative to native individuals in a focal environment. Finally, we close by benchmarking adaptive differentiation of *X*-linked and autosomal genes relative to differentiation of neutrally evolving loci.

Adaptive differentiation in the two-population model

To quantify adaptive differentiation between the two populations of the Moran model (Moran 1959, 1962), we used the fixation index:

$$F_{ST}^{i} = \frac{{\delta_i}^2}{4\hat{q}_i(1 - \hat{q}_i)}, \tag{11}$$

where δ_i is the equilibrium allele frequency difference between populations, $\hat{q}_i$ is the overall equilibrium allele

frequency for the A allele (*i.e.*, averaged between populations), and i refers to the inheritance mode ($i = \{A, X\}$). Equation 11 was evaluated using relevant expressions from Equations 5–7. In the following results, we present the ratio of F_{ST} at X-linked relative to autosomal loci, denoted F_{ST}^X/F_{ST}^A.

Consider the simplest scenario where adaptive alleles have additive fitness effects. In this case, differential contributions of the X and autosomes to local adaptation are minimized when migration is weak relative to the strength of selection for population differentiation (see Figure 2, left panel). Under weak migration (*i.e.*, $d \to 0$), each allele approaches fixation where it is favored ($F_{ST} \to 1$), and F_{ST}^X/F_{ST}^A approaches one. As the rate of migration increases, differentiation between populations becomes more pronounced on the X relative to the autosomes, provided there is some migration through males ($F_{ST}^X/F_{ST}^A > 1$ when $d_m > 0$; see Figure 2, left panel); the discrepancy between the X and autosomes becomes amplified with higher migration in males than females ($d_m > d_f$). The extent of population divergence on the X and autosomes, while dependent on the sex-averaged strength of selection, is unaffected by sex differences in selection.

To explore the impact of dominance on genetic differentiation at X-linked and autosomal genes, we developed extended results for each model of dominance described above (dominance reversal and parallel dominance), assuming high migration relative to selection ($d \gg s$; F_{ST}^X/F_{ST}^A again converges to one under weak migration). Overall, dominance has a relatively minor influence on the relative contribution of the X and autosomes to divergence. For the dominance reversal scenario, h has no effect at all, and in this case the additive results remain applicable (see Figure 2 and Figure S1). Similar results emerge from the parallel dominance model, though in this case the magnitude of large-X effects are somewhat dampened by deviations from additivity [F_{ST}^X/F_{ST}^A declines as $h(1 - h) \to 0$], particularly so when selection is stronger in males than females (see Figure S1). This latter result emerges from the effect of parallel dominance on the denominator of the F_{ST} equation [$4q_i(1 - q_i)$ in Equation 11]. Parallel dominance leads to unequal equilibrium frequencies of the pair of alleles, which decreases $q_i(1 - q_i)$ and inflates F_{ST}. This effect is dampened under X-linked inheritance, because selection in males promotes relatively equal equilibrium frequencies of A and B alleles [from Equation 7, a and c, $q_X(1 - q_X) > q_A(1 - q_A)$ when $s_m > 0$; otherwise, $q_X = q_A = 1/2$].

X-linked and autosomal allele frequency clines

In keeping with theoretical and empirical traditions in cline research, we consider the relative responses of X-linked *vs.* autosomal loci to local selection by calculating cline slopes of X-linked relative to autosomal genes across the environmental transition (*i.e.*, the ratio of maximum cline slopes, y_X/y_A). For both dominance scenarios, the X responds more efficiently than the autosomes to spatially variable selection over most of the parameter space of dominance, sex-specific selection, and migration (Figure 3). In the simplest case of additive fitness effects ($h = 1/2$), the ratio of cline slopes reduces to:

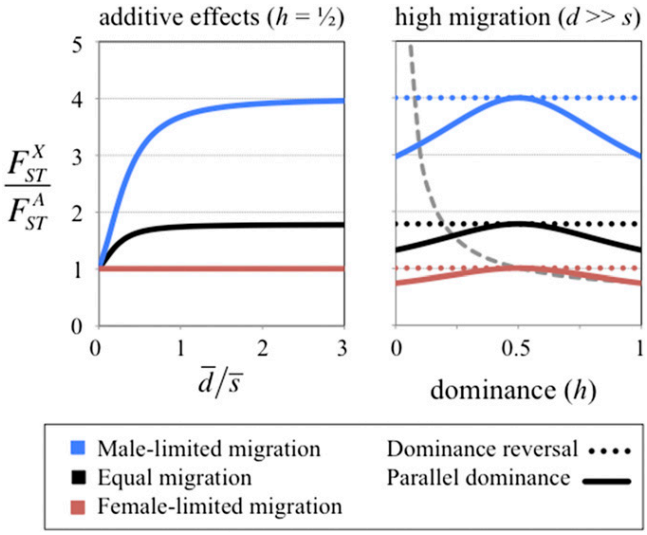

Figure 2 Adaptive divergence under migration-selection balance in the Moran, two-population model. The left panel (based on Equations 5, a and b, and 11) shows how the strength of migration relative to selection influences the ratio of differentiation at X-linked *vs.* autosomal loci. The x-axis shows the sex-averaged migration rate relative to the sex-averaged strength of selection: $\bar{d}/\bar{s} = (d_f + d_m)/(s_f + s_m)$. The right panel (based on Equations 6, 7, and 11) shows the effects of dominance on the ratio of differentiation at X-linked *vs.* autosomal loci, with equal selection in females and males ($s_f = s_m$; for the cases of male-limited and female-limited selection, see Figure S1). For point of reference, the dashed, gray line shows the relative rate of adaptive substitution on the X compared to the autosomes, as predicted by Charlesworth *et al.* [1987; from their equation 2a, the ratio of adaptive substitutions on the X relative to autosomes is $R = (1 + 2h)/(4h)$, dashed black line]. The dominance coefficient (h) is defined as $h = h_1 = h_2$ in the dominance reversal case, $h = h_1 = 1 - h_2$ under parallel dominance (see Table 1), and h as the dominance of beneficial mutations in the Charlesworth *et al.* (1987) model.

$$\frac{y_X}{y_A} = \sqrt{1 + \frac{m_m}{2m_f + m_m}}. \tag{12}$$

As in the two-population context, the relative contribution of the X to local adaptation in a cline becomes maximized under male-limited migration ($y_X/y_A = \sqrt{2} \approx 1.414$ when $m_f/m_m = 0$), and minimized under female-limited migration ($y_X/y_A = 1$ when $m_m/m_f = 0$). With equal migration of each sex, $y_X/y_A = \sqrt{(4/3)} \approx 1.15$. This set of results remains applicable under parallel dominance conditions (Figure 3). For the dominance reversal case, the ratio of cline slopes becomes marginally dependent on sex-specific selection and dominance conditions. Nevertheless, sex-specific migration patterns remain the dominant driver of differences between the X and autosomes (see Figure 3).

Clinal divergence of allele frequencies can also be expressed using F_{ST} metrics between populations that are located on opposite sides of the environmental transition (*i.e.*, between populations at locations x and $-x$, where $x = 0$ is

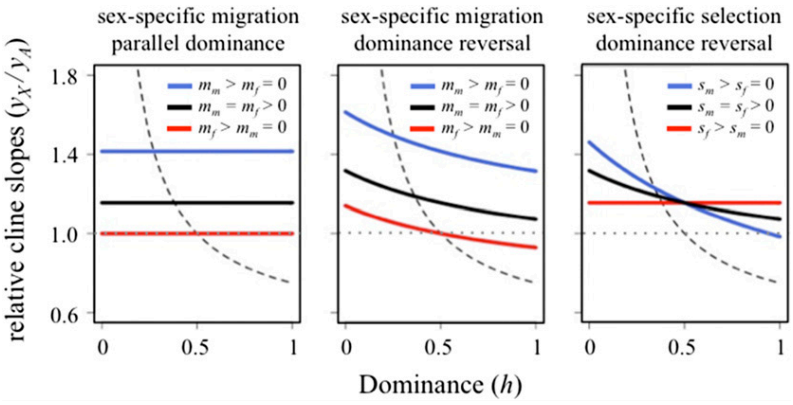

Figure 3 The effects of sex-specific selection, sex-biased migration, and dominance on the relative rates of clinal divergence at *X*-linked and autosomal loci. Solid curves are based on the analytical results from Equations 8 and 9. The first and second panels show the effects of sex-specific migration (m_f and m_m in females and males, respectively; selection is equal between the sexes) on the evolution of *X*-linked and autosomal clines. The third panel shows the effects of sex-specific selection (s_f and s_m in females and males; migration is equal between the sexes). For point of reference, the dashed line shows the relative rate of adaptive substitution on the *X* compared to the autosomes, as predicted by Charlesworth *et al.* [1987; from their equation 2a, the ratio of adaptive substitutions on the *X* relative to autosomes is $R = (1 + 2h)/(4h)$, dashed black line]. The dominance coefficient (h) is defined as $h = h_1 = h_2$ in the dominance reversal case, $h = h_1 = 1 - h_2$ under parallel dominance (see Table 1), and h as the dominance of beneficial mutations in the Charlesworth *et al.* (1987) model.

the point of transition). For populations far removed from the environmental transition (*i.e.*, far enough that the locally maladapted allele is eliminated, or nearly so), F_{ST} for the *X*, the autosomes, and their ratio approaches one. For subpopulations close to the environmental transition, we can revisit the additive effects model from above ($h = 1/2$) and quantify divergence between nearby subpopulations (at positions x and $-x$, where x approaches the environmental transition point) using the expressions:

$$F_{ST}{}^{A} \approx (2x)^2 \frac{s_\mathrm{m} + s_\mathrm{f}}{6(m_\mathrm{f} + m_\mathrm{m})} \tag{13a}$$

for an autosomal locus, and:

$$F_{ST}{}^{X} \approx (2x)^2 \frac{s_\mathrm{m} + s_\mathrm{f}}{3(2m_\mathrm{f} + m_\mathrm{m})} \tag{13a}$$

for an *X*-linked locus (see Appendix B). The ratio of F_{ST} for *X*-linked and autosomal loci simplifies to the square of the ratio of cline slopes, $F_{ST}^X/F_{ST}^A = (y_X/y_A)^2$, which reaches a maximum of two under male-limited migration.

Stepping-stone clines under gradual environmental change and genetic drift

The analytical models provide a baseline set of expectations regarding the relative role of the *X* chromosome in local adaptation along a cline. On the other hand, their results are restrictive by relying on two critical assumptions. First, they assume that the environmental transition is abrupt, which excludes the likely possibility of gradual environmental change across the species' range. Second, the results ignore impacts of population size, which are known to affect the relative rates of *X*-to-autosome adaptive substitution between species (Vicoso and Charlesworth 2009). To relax both assumptions, we carried out simulations using a stepping-stone model with H demes along a one-dimensional geographic axis. When possible, we have chosen parameter values of migration and selection to facilitate direct comparisons between simulated and analytical results (*e.g.*, $m > s$; see above for comments regarding comparisons between models).

Abrupt vs. gradual environmental change: We compared simulated outcomes from two distinct selection models: (1) an abrupt change model, which corresponds to the scenario used in the analytical results; and (2) a gradual change model, in which the intensity of selection gradually increases with distance from the range center (see Figure 1, middle and right panels, Table 1, and Table 2; the gradual change model corresponds to the "ramping" scenario described in Felsenstein 2015). Although there are some quantitative differences in the equilibrium clines of the two models—with large-*X* effects dampened under the ramping scenario—in general, we observed similar patterns of spatial divergence at *X*-linked and autosomal loci for the two forms of environmental change (Figure 4).

Effective population size and the ratio of X and autosome adaptive divergence: To investigate the sensitivity of the deterministic results to genetic drift, we carried out stochastic (Wright–Fisher) simulations that include selection, migration, and multinomial sampling of genotypes among the breeding adults in each subpopulation (see *Model* section above). These stochastic results deviated from deterministic predictions when the strength of selection was effectively weak (*i.e.*, when $N_e s$ was small, where N_e is the local effective population size and s is the sex-averaged strength of selection; see Figure 5). Under neutrality ($N_e s = 0$), the amount of spatial divergence was similar for the *X* and autosomes when each had a similar effective population size (*e.g.*, $N_{eX}/N_{eA} = 1$). A lower *X*-linked effective population size ($N_{eX}/N_{eA} < 1$) amplified the effects of genetic drift at *X*-linked loci, resulting in excess neutral divergence on the *X* and higher *X*-to-autosome divergence ratios than expected under deterministic selection without drift. Disparities between the stochastic and deterministic predictions declined rapidly with increasing

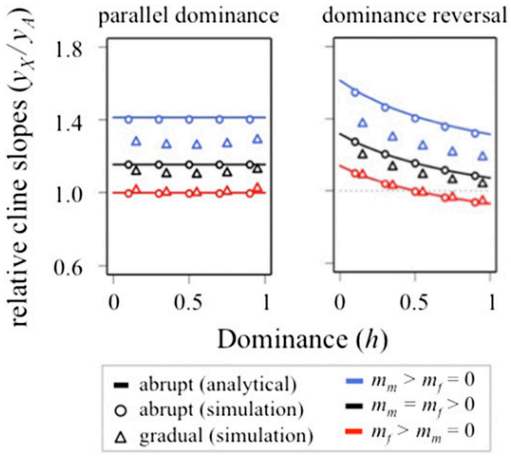

Figure 4 Relative rates of local adaptation on the *X* and autosomes: comparison between analytical and stepping-stone models under abrupt and gradual environmental change. Analytical results (solid curves) are based on Equations 7 and 10. ○ and △ show the results of deterministic forward simulations of the stepping-stone model, under an abrupt (○; Table 1) or gradual (△; Table 2) environmental transition. Results are presented for three migration scenarios: male-limited migration (blue), female-limited migration (red), and equal migration between the sexes (black). Parameters were $m = (m_m + m_f)/2 = 0.1$, $s = (s_m + s_f)/2 = 0.002$, and $H = 100$ habitats in the stepping-stone model.

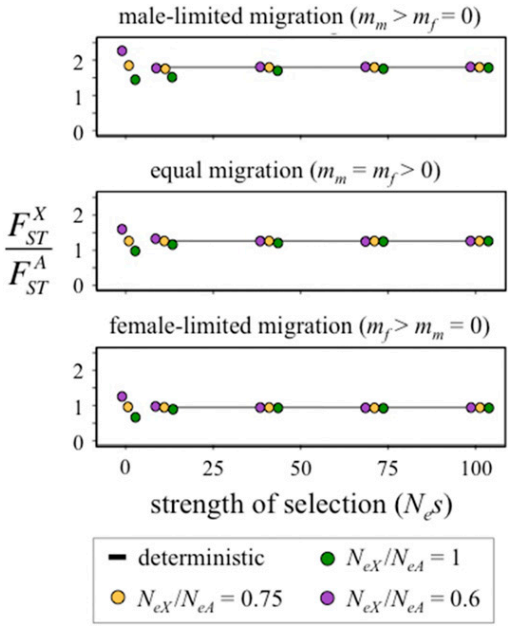

Figure 5 Influence of effective population size on genetic divergence between adjacent demes in the stepping-stone model. Results show the maximum values of F_{ST}^X and F_{ST}^A between pairs of adjacent demes along the gradient (*i.e.*, the maximum of $H - 1$ pairwise F_{ST} values). Results that track F_{ST} at the center of the species range (*i.e.*, across the environmental transition) are indistinguishable. Each panel compares deterministic forward simulations (gray line) against stochastic simulations for different ratios of *X*-linked to autosome effective population size (N_{eX}/N_{eA}). The effective strength of selection ($N_e s$) refers to the product of local population size [$N = N_{eA} = 4N_f N_m/(N_f + N_m)$] and the selection coefficient ($s = s_f = s_m = 0.05$). Parameters were set to $h = 0.5$, $m = (m_m + m_f)/2 = 0.1$, and $H = 30$ habitats in the stepping-stone model.

effective strength of selection (increasing $N_e s$; Figure 5). When selection is effectively strong ($N_e s > \sim 10$), predictions from the deterministic models are robust to differences in the *relative* population sizes of *X*-linked and autosomal loci.

Relative contribution of the X and autosomes to the fitness load of migrants

The results above can be used to quantify the relative contributions of *X*-linked and autosomal loci to the fitness load of migrant relative to native individuals of a population. For simplicity, we focus on the additive case ($h = 1/2$) and quantify the fitness load (fitness of migrants relative to natives) as:

$$L = \frac{\bar{w}_N - \bar{w}_M}{\bar{w}_N}, \tag{14}$$

where $\bar{w}_N$ and $\bar{w}_M$ represent the mean fitness of native and migrant individuals, respectively, within a focal habitat.

From Equation 14, we can quantify the relative contribution of an *X*-linked and autosomal locus to the migrant fitness load; assuming that each locus has a fitness effect of s_j in the *j*th sex (see Appendix C). In the two-population model, the relative load on the *X* and autosomes simplifies to $L_X/L_A = \sqrt{F_{ST}^X/F_{ST}^A}$, which (given the results presented above, *e.g.*, Figure 2) falls within the range $1 < L_X/L_A < 2$. Using a similar approach to the cline context, we can quantify the load of individuals born slightly above the environmental transition (from location x; $1 \gg x > 0$) that migrate to just below the transition (to location $-x$). In this case, the relative load on the *X* and autosomes simplifies to $L_X/L_A = y_X/y_A$. From above (*e.g.*, Figure 3), this falls within the range $1 < L_X/L_A < \sqrt{2}$.

Population differentiation at selected relative to neutral loci

The theory presented above predicts that the *X* will contribute disproportionately to local adaptation under a broad set of biological conditions (*i.e.*, when there is appreciable migration of the heterogametic sex). On the other hand, genetic drift accounts for population differentiation at most loci within a genome, and identifying differentially selected loci against this genomic background of neutral divergence represents a major challenge in population genomics (Hoban *et al.* 2016). One approach for identifying candidate loci under local selection is to establish a neutral distribution of F_{ST} (*e.g.*, based on genome-wide polymorphism data) and subsequently target outlier loci that fall outside the neutral range; outlier loci represent candidate genes responding to local selection (Lewontin and Krakauer 1973). This approach poses a challenge in the context of *X vs.* autosome comparisons, because the distribution of neutral F_{ST} can systematically differ between chromosomes (*e.g.*, Laporte and Charlesworth 2002; Hedrick 2007), leading to different opportunities to identify candidate loci responding to local selection. Because the breadth of the distribution of neutral F_{ST} will often be greater on the *X* than the autosomes (*e.g.*, due to

reduced N_e for *X*-linked genes and/or male-biased migration), it may be more difficult to reliably identify outlier F_{ST} loci on the *X* despite elevated contributions of *X*-linked genes to local adaptation.

We can apply the theory of neutral F_{ST} to establish a theoretical baseline of neutral population differentiation on the *X* and the autosomes, and classify scenarios in which outlier F_{ST} analysis will identify *X*-linked and autosomal candidate loci for local adaptation. We focus our attention on F_{ST} between a pair of populations with high levels of migration and low neutral F_{ST}, leading to relatively promising conditions for identifying selected loci with F_{ST} above the neutral range. Following standard theory (*e.g.*, Slatkin 1991; Laporte and Charlesworth 2002) and assuming effectively strong migration on both the *X* and autosomes (specifically, $N_{ei}m_i \gg 1 \gg m_i$, where N_{ei} and m_i represent the effective population size and effective migration rate for inheritance system $i = \{A, X\}$), the expected F_{ST} on the *X* relative to the autosomes is:

$$\frac{E(F_{ST}{}^X)}{E(F_{ST}{}^A)} \approx \frac{N_{eA}m_A}{N_{eX}m_X} = \frac{3N_{eA}}{4N_{eX}} \cdot \frac{2(m_f + m_m)}{(2m_f + m_m)}. \quad (15)$$

Based on Equation 15, mean neutral divergence on the *X* exceeds that of the autosomes under broad conditions of effective population size (*e.g.*, $N_{eX}/N_{eA} < 1$) and sex-biased migration (*e.g.*, $m_m/m_f > 0$) (see Figure S2). Nevertheless, the excess adaptive differentiation on the *X* relative to autosomes (described above) is often higher than the *X vs.* autosome differences at neutral loci. For example, in the two-population model with additive fitness effects and strong migration relative to selection, the *X*-to-autosome F_{ST} ratio at selected loci will be greater than the ratio of mean neutral F_{ST} (Equation 15) as long as the following condition is true:

$$\frac{N_{eX}}{N_{eA}} > \frac{3(2m_f + m_m)}{8(m_f + m_m)}. \quad (16a)$$

The condition is always met when $N_{eX}/N_{eA} > 0.75$, and the criterion for excess divergence at selected loci becomes more permissive with higher male than female migration (*i.e.*, $m_m/m_f > 1$). In the cline models at the species' range center (and under the same assumptions as above, *i.e.*: $h = 1/2$; $m \gg s$), the criterion for a higher *X*-to-autosome F_{ST} ratio at selected relative to neutral loci is:

$$\frac{N_{eX}}{N_{eA}} > \frac{3}{4}. \quad (16b)$$

To quantify opportunities for selected loci on the *X* and autosomes to reach outlier status, we simulated the distribution of neutral F_{ST} for *X*-linked and autosomal loci (each based on 10,000 simulated neutral loci) in the two-population model of population subdivision. We then calculated the fraction of nonneutral loci at which selection is sufficiently strong to drive F_{ST} beyond the 95th percentile tail of the neutral F_{ST} distribution, per chromosome. We assumed an exponential distribution of selection coefficients at selected loci, with identical fitness effect distributions among loci on the *X* and autosomes. These simulations show that Equation 16a provides a useful benchmark for the relative fraction of selected loci that reach outlier status on the *X* and autosomes (Figure 6; where the *X* has a higher fraction of outlier loci than the autosomes when Equation 16a is true). In general, the *X* exhibits an excess of outliers relative to the autosomes, despite its tendency for higher neutral F_{ST} (Figure 6). The discrepancy in the number of outlier loci on the *X* and autosomes is sensitive to the average fitness effect of selected loci, $E(s)$. As $E(s)$ decreases in magnitude, a smaller fraction of selected loci reach outlier status on both chromosome types, but the relative fraction reaching outlier status becomes more asymmetrical between chromosomes (*e.g.*, to the left of each *x*-axis of Figure 6).

Discussion

The theory presented here predicts that the *X* chromosome (as well as the *Z* in species with female-heterogametic sex determination) will make a disproportionately large contribution to adaptive genetic differentiation between populations that are connected through gene flow. In contrast to theories of faster-*X* divergence between species (see Vicoso and Charlesworth 2006; Meisel and Connallon 2013), the outsized contribution of the *X* to local adaptation is relatively insensitive to sex-biased natural selection, genetic dominance, or effective population size. Instead, the magnitude of the large-*X* effect in local adaptation hinges upon the relative rate of migration in females and males. High rates of migration within the heterogametic sex (*i.e.*, males in species with an *X*; females in species with *Z* chromosomes) elevate the relative contribution of sex-linked genes to adaptive differentiation between subpopulations of a species.

In the following sections, we address three biological implications of the new theory. We first outline the major points of difference between spatial and temporal models of *X* and autosome evolution; we dissect the distinct biological conditions that give rise to large-*X* effects in adaptation across spatial *vs.* temporal scales. Second, we outline challenges and potential approaches for testing the theory. We emphasize that—while few studies to date have examined the contributions of the *X* and autosomes to local adaptation—the theory presented here provides a useful roadmap for future empirical research in the arena of local adaptation. Third, we provide an overview of limitations of our models, where each justifies future theoretical work on the population genetics of *X*-linked adaptation within structured populations.

Contributions of the X to local adaptation vs. long-term adaptive divergence

Evolutionary scenarios of spatial and temporal divergence follow distinct theoretical traditions, and use distinct modeling approaches. The theory of local adaptation on the *X* and autosomes, presented here, is most readily compared to a

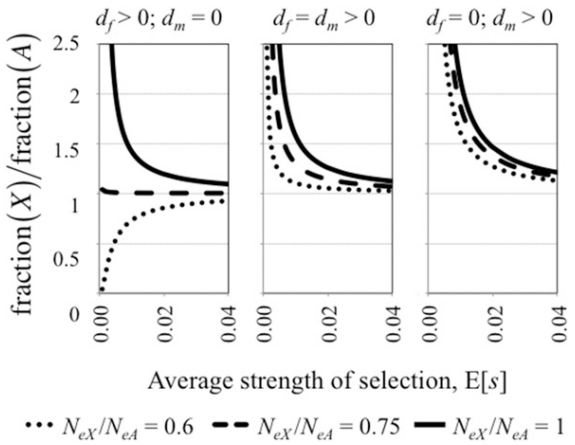

Figure 6 Outlier status of *X*-linked and autosomal loci in the two-population model. The curves show the relative fraction of selected loci that fall within the upper 95th percentile tail of the neutral distribution of F_{ST}. Three scenarios of migration are shown: female-limited migration ($d_f > 0$; $d_m = 0$), equal migration ($d_f = d_m > 0$); and male-limited migration ($d_f = 0$; $d_m > 0$). Neutral F_{ST} distributions, including 95th percentile thresholds, were obtained by simulating 10,000 neutral loci for each chromosome and each scenario of N_{eX}/N_{eA}. Results are shown for the specific case of $N_{eA} = 5000$ and $(m_f + m_m)/2 = 0.1$. Additional results, using larger effective population sizes and smaller migration rates, are presented in File S1. Deterministic equations for F_{ST} under selection and additive fitness effects were used to quantify the fractions of selected loci that reach the 95th percentile threshold of neutral loci, and assuming that selection coefficients [*i.e.*, $s = (s_f + s_m)/2$] are exponentially distributed with a mean of $E(s)$ under each mode of linkage.

well-developed theory on the relative rate of adaptive substitutions at *X*-linked and autosomal genes (faster-*X* theory). Below, we discuss two prominent points of contrast between these theories.

In the faster-*X* theory, the *X* adapts more rapidly than the autosomes when beneficial mutations are, on average, partially or completely recessive, which reflects the inflated fixation probabilities of rare beneficial mutations on the *X* (*e.g.*, Avery 1984; Charlesworth *et al.* 1987; but see Vicoso and Charlesworth 2009). In contrast, the new theory reveals a modest effect of dominance in contexts of local adaptation (*e.g.*, Figure 2 and Figure 3). This insensitivity to dominance arises from a simple cause. Divergence under gene flow depends primarily on the rate of evolutionary response to selection on intermediate-frequency alleles, as opposed to fixation probabilities of rare mutations. Dominance has a reduced impact on the response to selection when alternative alleles at a locus are both common within a population. And, in the absence of any major effects of dominance on *X*-linked and autosome evolutionary dynamics, the tendency of the *X* to diverge more extensively than autosomes reflects its inherently greater responsiveness to natural selection (regardless of dominance)—a feature that has long been recognized by population genetics theory (see Avery 1984).

The relative rates of *X*-to-autosome adaptive substitution are also sensitive to the effective population sizes of *X*-linked and autosomal genes (N_{eX} and N_{eA}, respectively), with large ratios of N_{eX}/N_{eA} enhancing faster-*X* effects (*i.e.*, $N_{eX}/N_{eA} > 0.75$) and small ratios dampening them (*i.e.*, $N_{eX}/N_{eA} < 0.75$) (see Vicoso and Charlesworth 2009). In contrast, the contribution of the *X* to local adaptation is relatively insensitive to effective population size, provided the overall efficacy of selection is strong (*e.g.*, $N_e s \gg 10$). This feature of local adaptation models once again reflects the importance of selection on common genetic variants. Effective population size plays a minor role in the dynamics of intermediate-frequency alleles, because effectively strong selection (large $N_e s$) gives rise to pseudodeterministic evolutionary dynamics of beneficial alleles (Barton 1998).

Empirical observations of distinct evolutionary dynamics of *X*-linked and autosomal genes potentially provide signals of sex-specific evolutionary processes, and may reveal features of the genetic basis of adaptation (Vicoso and Charlesworth 2006; Meisel and Connallon 2013). Given the fundamental differences between spatial and temporal scenarios of adaptation, large-*X* effects in local adaptation and faster-*X* patterns of adaptive substitution reveal fundamentally distinct features of the evolutionary genetics of adaptation. Whereas faster-*X* effects emerge from genetic constraints that limit rates of adaptation (*i.e.*, Charlesworth *et al.* 1987; Orr and Betancourt 2001; Orr 2010; Connallon *et al.* 2012); large-*X* effects in local adaptation arise from intrinsic properties of *X*-chromosome transmission, and reflect adaptive constraints imposed by gene flow between divergently selected populations.

Testing for a large-X effect in local adaptation

By generating new predictions about the evolutionary genetic basis of local adaptation, the new theory provides a strong motivation to empirically quantify the roles of *X*- and *Z*-linked genes in local adaptation. Below, we outline two complementary approaches for testing the theory.

The most straightforward approach is to directly map the genetic basis of traits that are known to have diverged under selection for local adaptation. This approach should be feasible in empirical systems, where controlled crosses can be carried out with relative ease and where traits subject to local selection may be measured with high replication and under standardized environmental conditions (*i.e.*, in the laboratory or greenhouse). Several crossing approaches can be taken to isolate effects of the *X* from other regions of the genome, and these range from relatively simple to complex (Reinhold 1998; Fairbairn and Roff 2006; Masly and Presgraves 2007). One obvious system where this direct mapping approach would apply is *Drosophila*, which shows predictable patterns of spatial divergence in response to environmental variation by latitude (Hoffmann and Weeks 2007; Sgrò *et al.* 2010). Geographically widespread plant species (with sex chromosomes) may also prove useful, with transplant experiments allowing for direct estimation of genotype-by-environment effects on fitness. While direct mapping strategies for partitioning *X*-linked effects on quantitative trait variation are widely

employed in studies on the genetic basis of species incompatibilities (where the focal trait is typically hybrid sterility or inviability; Coyne and Orr 1989), this approach has not, to our knowledge, been used to examine the role of the *X* in local adaptation.

Genomics offers an alternative and indirect approach to test for a large-*X* effect in local adaptation by way of F_{ST} outlier analysis. As we show above, such indirect approaches must deal with the challenge of identifying differentially selected *X*-linked loci against a background of neutral F_{ST} that is typically elevated relative to autosomal loci. Nevertheless, our simulations provide some indications about the study systems in which genomic approaches are most, and least, likely to bear fruit. One key factor is the relative effective population sizes of *X*-linked and autosomal genes, with high N_{eX}/N_{eA} ratios (*e.g.*, near one) providing the most balanced context to test for F_{ST}-outlier differences between chromosomes. We now have access to empirical estimates of this ratio in a reasonably large number of taxa and, in general, it appears that N_{eX}/N_{eA} ratios are typically higher in male-heterogametic than female-heterogametic species (Mank *et al.* 2010; Vicoso *et al.* 2013; Sackton *et al.* 2014; Huang and Rabosky 2015). Mammals and insects (excluding Trichoptera and Lepidoptera) may therefore represent the best systems for testing the theory. Sex-biased migration through the heterogametic sex amplifies large-*X* effects in local adaptation and elevates genomic signals of the effect in species with simple population structures (as in the two-population model, above; Figure 6). A recent meta-analysis of sex-biased migration in animals includes several species that would be suitable to test the new theory (see Trochet *et al.* 2016). While few studies have evaluated spatial patterns of *X*-linked *vs.* autosomal adaptive divergence at the genomic level, we tentatively point to one empirical example that appears to support our theoretical predictions. The human *X* chromosome is enriched for SNPs that are highly differentiated among global subpopulations; these highly divergent loci represent excellent candidates for adaptive divergence to local environmental conditions (Lambert *et al.* 2010).

In contrast to the deficit of research on the *X* in local adaptation, many studies have considered the effects of *X*-linkage on gene flow between hybridizing species. There is strong evidence of constrained interspecific gene flow on the *X* (see Muirhead and Presgraves 2016 and citations therein), yet the driver of this reduction in *X*-linked gene flow is likely to differ from those that elevate the role of the *X* in local adaptation. As recently shown by Muirhead and Presgraves (2016), the dominance of reproductive incompatibilities in interspecific hybrids represents the single *most* important factor in maintaining *X*-linked and autosome clines across hybrid zones. Hybrid genetic incompatibilities, which generally appear to be recessive, generate large-*X* effects on hybrid incompatibilities (see Masly and Presgraves 2007; Muirhead and Presgraves 2016). These findings highlight that, while large-*X* effects arise at several scales of evolutionary divergence between populations and species (*e.g.*, from local adaptation, to reproductive isolation, to adaptive divergence between species), these effects likely owe their origins to different evolutionary genetic causes.

Theoretical limitations and future directions

We considered the evolution of allele-frequency divergence on the *X* and autosomes within two simple contexts of geographic subdivision (*i.e.*, between a pair of equally sized subpopulations, and among subpopulations spread linearly across a spatial axis). The models reveal new insights into the genomic basis of local adaptation, including a special role for the *X* chromosome. Nevertheless, there remains considerable scope for additional theory regarding the effects of *X*-linkage on adaptation across a species' range. We consider three potential extensions, below.

First, we modeled evolutionary dynamics under static population demography, and thus excluded feedbacks between evolutionary and demographic change. This approach is generally reasonable for simple genetic (*e.g.*, single-locus) models with small selection coefficients, yet eco-evolutionary feedbacks could be important in contexts of strong selection at single loci or in models of selection on polygenic quantitative traits. Extensions of the theory to cases of polygenic adaptation with eco-evolutionary feedbacks could represent an interesting area for future study and, to our knowledge, there is currently no theory that explicitly considers *X*-chromosome dynamics in the context of eco-evolutionary feedbacks. Such studies could build upon extensive prior theory from evolutionary quantitative genetics (*e.g.*, Lande 1980; Garcia-Ramos and Kirkpatrick 1997; Kirkpatrick and Barton 1997; Polechová and Barton 2015).

We also focused exclusively on equilibrium patterns of population divergence, and thereby ignored interesting features of the nonequilibrium dynamics of *X* and autosome evolution. For example, recent work by Ralph and Coop (2010, 2015) highlights the potential for "parallel" adaptation between populations that are partially isolated, geographically. In this context, each allele that is unequivocally beneficial across the entire species' range may either arise once within the species range and subsequently spread to all the subpopulations; or it may arise independently in multiple regions of the range, leading to geographically unique genetic pathways to adaptation to a shared evolutionary challenge. From existing theory, we know that the probability of each pathway to adaptation depends on the rate of migration relative to the strength of mutation and selection. Each of these factors can potentially differ between the *X*-linked and autosomal loci by way of sex-specific processes of selection, mutation, migration, and drift. Future models may therefore consider whether and when probabilities of parallel adaptation differ between the *X* and autosomes—a question that carries implications for empirical tests of recent selection (*e.g.*, Messer and Petrov 2013) and efforts to map the genetic basis of adaptive phenotypes (Tishkoff *et al.* 2007).

Finally, we presented a first examination of the potential to observe excess outlier F_{ST} loci on the *X* relative to the genomic distribution of F_{ST} at neutrally evolving loci. While these results are useful for identifying empirical systems amenable to testing the new theory, the approach could be taken much further. For example, we focused on the simplest forms of stable population structure, leaving considerable room for future explorations of *X*-linked and autosomal diversity under more complex population structures and histories (*e.g.*, Whitlock and Lotterhos 2015; Hoban *et al.* 2016), including recent population expansions or contractions that may differentially affect the *X* and autosomes (Pool and Nielsen 2007). Effects of hitchhiking and background selection may likewise influence neutral diversity in structured populations (Zeng and Corcoran 2015), and the effects of each are likely to differ between the *X* and autosomes (Betancourt *et al.* 2004; Charlesworth 2012). The combined effects of linked selection, population structure, and *X*-linked inheritance have yet to be considered by theory, and this also represents an interesting area for future work.

Conclusions

Theory has long predicted distinct population genetic dynamics at *X*-linked and autosomal genes (*e.g.*, Haldane 1924; Avery 1984; Charlesworth *et al.* 1987; reviewed in Vicoso and Charlesworth 2006 and Hedrick 2007). These predictions have become increasingly prominent in evolutionary genetics research over the last two decades, as a result of growing appreciation of the importance of sex chromosomes in species diversification (Coyne and Orr 1989; Presgraves 2008), and as rapidly advancing genome sequencing technology has made evolutionary contrasts between the *X* and autosomes increasingly feasible (Vicoso and Charlesworth 2006; Presgraves 2008; Meisel and Connallon 2013). While empirical and theoretical research on *X*-linked and autosomal evolutionary dynamics has traditionally focused on patterns of polymorphism in single populations (Charlesworth 2009) and evolutionary divergence between species (Presgraves 2008; Meisel and Connallon 2013), it has largely overlooked the potential role of the *X* chromosome in local adaptation (for exceptions see: Owen 1986; Nagylaki 1996; Parker and Hedrick 2000). Our models provide new motivation to quantify the relative contributions of the *X* and autosomes to geographic differentiation across species' ranges.

Acknowledgments

We are grateful to Colin Olito for helping to speed up the simulations, and to Brian Charlesworth, Matt Hall, and an anonymous reviewer for valuable comments and suggestions on an earlier version of the manuscript. Support for this research was provided by the School of Biological Sciences at Monash University and the Australian Research Council.

Literature Cited

Avery, P., 1984 The population genetics of haplo-diploids and X-linked genes. Genet. Res. 44: 321–341.

Barton, N. H., 1998 The effect of hitch-hiking on neutral genealogies. Genet. Res. 72: 123–133.

Berg, L. M., M. Lascoux, and P. Pamilo, 1998 The infinite island model with sex- differentiated gene flow. Heredity 81: 63–68.

Betancourt, A. J., Y. Kim, and H. A. Orr, 2004 A pseudohitchhiking model of X *vs.* autosomal diversity. Genetics 168: 2261–2269.

Charlesworth, B., 1992 Evolutionary rates in partially self-fertilizing species. Am. Nat. 140: 126–148.

Charlesworth, B., 2009 Fundamental concepts in genetics: effective population size and patterns of molecular evolution and variation. Nat. Rev. Genet. 10: 195–205.

Charlesworth, B., 2012 The role of background selection in shaping patterns of molecular evolution and variation: evidence from variability on the Drosophila X chromosome. Genetics 191: 233–246.

Charlesworth, B., and D. Charlesworth, 2010 *Elements of Evolutionary Genetics*. Roberts and Company Publishers, Greenwood Village, CO.

Charlesworth, B., J. A. Coyne, and N. H. Barton, 1987 The relative rates of evolution of sex chromosomes and autosomes. Am. Nat. 130: 113–146.

Connallon, T., N. D. Singh, and A. G. Clark, 2012 Impact of genetic architecture on the relative rates of X *vs.* autosomal adaptive substitution. Mol. Biol. Evol. 29: 1933–1942.

Coyne, J. A., and H. A. Orr, 1989 Two rules of speciation, pp. 180–207 in *Speciation and Its Consequences*, edited by D. Otte, and J. Endler. Sinauer Associates, Sunderland, MA.

Curtsinger, J. W., P. M. Service, and T. Prout, 1994 Antagonistic pleiotropy, reversal of dominance, and genetic polymorphism. Am. Soc. Nat. 144: 210–228.

Fairbairn, D. J., and D. A. Roff, 2006 The quantitative genetics of sexual dimorphism: assessing the importance of sex-linkage. Heredity 97: 319–328.

Felsenstein, J., 1976 The theoretical population genetics of variable selection and migration. Annu. Rev. Genet. 10: 253–280.

Felsenstein, J., 2015 Theoretical evolutionary genetics. Free e-book. Available at: http://evolution.genetics.washington.edu/pgbook/pgbook.html. Accessed December 2015.

Fisher, R. A., 1950 Gene frequencies in a cline determined by selection and diffusion. Biometrics 6: 353–361.

Fry, J. D., 2010 The genomic location of sexually antagonistic variation: some cautionary comments. Evolution. 64: 1510–1516.

Garcia-Ramos, G., and M. Kirkpatrick, 1997 Genetic models of adaptation and gene flow in peripheral populations. Evolution 51: 21–28.

Gillespie, J. H., 1991 *The Causes of Molecular Evolution*. Oxford University Press, New York.

Gillespie, J. H., 2004 *Population Genetics: A Concise Guide*. Johns Hopkins University Press, Baltimore.

Glémin, S., and J. Ronfort, 2013 Adaptation and maladaptation in selfing and outcrossing species: new mutations *vs.* standing variation. Evolution. 67: 225–240.

Haldane, J. B. S., 1924 A mathematical theory of natural and artificial selection. Part I. Trans. Camb. Philos. Soc. 23: 19–41.

Haldane, J. B. S., 1948 The theory of a cline. J. Genet. 48: 276–284.

Hartl, D. L., and A. G. Clark, 2007 *Principles of Population Genetics*, Ed. 4. Sinauer Associates, Sunderland, MA.

Hedrick, P. W., 1986 Genetic polymorphism in heterogeneous environments: a decade later. Annu. Rev. Ecol. Syst. 17: 535–566.

Hedrick, P. W., 2006 Genetic polymorphism in heterogeneous environments: the age of genomics. Annu. Rev. Ecol. Evol. Syst. 37: 67–93.
Hedrick, P. W., 2007 Sex: differences in mutation, recombination, selection, gene flow, and genetic drift. Evolution 61: 2750–2771.
Hedrick, P. W., M. E. Ginevan, and E. P. Ewing, 1976 Genetic polymorphism in heterogeneous environments. Annu. Rev. Ecol. Syst. 7: 1–32.
Hermisson, J., and P. S. Pennings, 2005 Soft sweeps: molecular population genetics of adaptation from standing genetic variation. Genetics 169: 2335–2352.
Hill, W. G., 1982 Predictions of response to artificial selection from new mutations. Genet. Res. 40: 255–278.
Hoban, S., J. L. Kelly, K. E. Lotterhos, M. F. Antolin, G. Bradburd *et al.*, 2016 Finding the genomic basis of local adaptation: pitfalls, practical solutions, and future directions. Am. Nat. 188: 379–397.
Hoffmann, A. A., and A. R. Weeks, 2007 Climatic selection on genes and traits after a 100 year-old invasion: a critical look at the temperate-tropical clines in *Drosophila melanogaster* from eastern Australia. Genetica 129: 133–147.
Huang, H., and D. L. Rabosky, 2015 Sex-linked genomic variation and its relationship to avian plumage dichromatism and sexual selection. BMC Evol. Biol. 15: 1–10.
Kidwell, J. F., M. T. Clegg, F. M. Stewart, and T. Prout, 1977 Regions of stable equilibria for models of differential selection in the two sexes under random mating. Genetics 85: 171–183.
Kirkpatrick, M., and N. H. Barton, 1997 Evolution of a species' range. Am. Nat. 150: 1–23.
Kirkpatrick, M., and D. W. Hall, 2004 Male-biased mutation, sex linkage, and the rate of adaptive evolution. Evolution 58: 437–440.
Lambert, C. A., C. F. Connelly, J. Madeoy, R. Qiu, M. V. Olson *et al.*, 2010 Highly punctuated patterns of population structure on the X chromosome and implications for African evolutionary history. Am. J. Hum. Genet. 86: 34–44.
Lande, R., 1980 Sexual dimorphism, sexual selection, and adaptation in polygenic characters. Evolution 34: 292–305.
Laporte, V., and B. Charlesworth, 2002 Effective population size and population subdivision in demographically structured populations. Genetics 162: 501–519.
Levene, H., 1953 Genetic equilibrium when more than one ecological niche is available. Am. Nat. 87: 331–333.
Lewontin, R. C., and J. Krakauer, 1973 Distribution of gene frequency as a test of the theory of the selective neutrality of polymorphisms. Genetics 74: 175–195.
Mank, J. E., B. Vicoso, S. Berlin, and B. Charlesworth, 2010 Effective population size and the faster-X effect: empirical results and their interpretation. Evolution. 64: 663–674.
Manna, F., G. Martin, and T. Lenormand, 2011 Fitness landscapes: an alternative theory for the dominance of mutation. Genetics 189: 923–937.
Martin, G., and T. Lenormand, 2006 The fitness effect of mutation across environments: a survey in light of fitness landscape models. Evolution 60: 2413–2427.
Martin, G., and T. Lenormand, 2008 The distribution of beneficial and fixed mutation fitness effects close to an optimum. Genetics 179: 907–916.
Martin, G., and T. Lenormand, 2015 The fitness effect of mutations across environments: Fisher's geometrical model with multiple optima. Evolution. 69: 1–36.
Masly, J. P., and D. C. Presgraves, 2007 High-resolution genome-wide dissection of the two rules of speciation in *Drosophila*. PLoS Biol. 5: 1890–1898.
McCandlish, D. M., and A. Stoltzfus, 2014 Modeling evolution using the probability of fixation: history and implications. Q. Rev. Biol. 89: 225–252.
Meisel, R. P., and T. Connallon, 2013 The faster-X effect: integrating theory and data. Trends Genet. 29: 537–544.
Messer, P. W., and D. A. Petrov, 2013 Population genomics of rapid adaptation by soft selective sweeps. Trends Ecol. Evol. 28: 659–669.
Moran, P. A. P., 1959 The theory of some genetical effects of population subdivision. Aust. J. Biol. Sci. 12: 109–116.
Moran, P. A. P., 1962 *The Statistical Processes of Evolutionary Theory.* Clarendon Press, Oxford.
Muirhead, C. A., and D. C. Presgraves, 2016 Hybrid incompatibilities, local adaptation, and the genomic distribution of natural introgression between species. Am. Nat. 187: 249–261.
Nagylaki, T., 1996 The diffusion model for migration and selection in a dioecious population. J. Math. Biol. 34: 334–360.
Orr, H. A., 1998 The population genetics of adaptation: the distribution of factors fixed during adaptive evolution. Evolution 52: 935–949.
Orr, H. A., 2002 The population genetics of adaptation: the adaptation of DNA sequences. Evolution 56: 1317–1330.
Orr, H. A., 2005 The genetic theory of adaptation: a brief history. Nat. Rev. Genet. 6: 119–127.
Orr, H. A., 2006 The distribution of fitness effects among beneficial mutations in Fisher's geometric model of adaptation. J. Theor. Biol. 238: 279–285.
Orr, H. A., 2010 The population genetics of beneficial mutations. Phil. Trans. R. Soc. B 365: 1195–1201.
Orr, H. A., and A. J. Betancourt, 2001 Haldane's sieve and adaptation from the standing genetic variation. Genetics 157: 875–884.
Owen, R. E., 1986 Gene frequency clines at X-linked or haplodiploid loci. Heredity 57: 209–219.
Parker, J. D., and P. W. Hedrick, 2000 Gene flow and selection balance in haplodiploid social insects. Heredity 85: 530–538.
Peischl, S., I. Dupanloup, M. Kirkpatrick, and L. Excoffier, 2013 On the accumulation of deleterious mutations during range expansions. Mol. Ecol. 22: 5972–5982.
Peischl, S., M. Kirkpatrick, and L. Excoffier, 2015 Expansion load and the evolutionary dynamics of a species range. Am. Nat. 185: 81–93.
Polechová, J., and N. H. Barton, 2015 Limits to adaptation along environmental gradients. Proc. Natl. Acad. Sci. USA 112: 6401–6406.
Pool, J. E., and R. Nielsen, 2007 Population size changes reshape genomic patterns of diversity. Evolution 61: 3001–3006.
Presgraves, D. C., 2008 Sex chromosomes and speciation in Drosophila. Trends Genet. 24: 336–343.
Prout, T., 2000 How well does opposing selection maintain variation? pp. 157–203 in *Evolutionary Genetics from Molecules to Morphology*, Cambridge University Press, Cambridge, United Kingdom.
R Core Team, 2014 R: A Language and Environment for Statistical Computing. R Foundation for Statistical Computing, Vienna, Austria.
Ralph, P., and G. Coop, 2010 Parallel adaptation: one or many waves of advance of an advantageous allele? Genetics 186: 647–668.
Ralph, P. L., and G. Coop, 2015 The role of standing variation in geographic convergent adaptation. Am. Nat. 186: S5–S23.
Reinhold, K., 1998 Sex linkage among genes controlling sexually selected traits. Behav. Ecol. Sociobiol. 44: 1–7.
Sackton, T. B., R. B. Corbett-detig, J. Nagaraju, L. Vaishna, K. P. Arunkumar *et al.*, 2014 Positive selection drives faster-Z evolution in silkmoths. Evolution 68: 2331–2342.
Sgrò, C. M., J. Overgaard, T. N. Kristensen, K. A. Mitchell, F. E. Cockerell *et al.*, 2010 A comprehensive assessment of geographic variation in heat tolerance and hardening capacity in populations of *Drosophila melanogaster* from Eastern Australia. J. Evol. Biol. 23: 2484–2493.

Slatkin, M., 1991 Inbreeding coefficients and coalescence times. Genet. Res. 58: 167–175.
Smith, J. M., 1970 Natural selection and the concept of a protein space. Nature 225: 563–564.
Tishkoff, S. A., F. A. Reed, A. Ranciaro, B. F. Voight, C. C. Babbitt *et al.*, 2007 Convergent adaptation of human lactase persistence in Africa and Europe. Nat. Genet. 39: 31–40.
Trochet, A., E. A. Courtois, V. M. Stevens, M. Baguette, A. Chaine *et al.*, 2016 Evolution of sex-biased dispersal. Q. Rev. Biol. 91: 297–320.
Vicoso, B., and B. Charlesworth, 2006 Evolution on the X chromosome: unusual patterns and processes. Nat. Rev. Genet. 7: 645–653.
Vicoso, B., and B. Charlesworth, 2009 Effective population size and the faster-X effect: an extended model. Evolution. 63: 2413–2426.
Vicoso, B., J. J. Emerson, Y. Zektser, S. Mahajan, and D. Bachtrog, 2013 Comparative sex chromosome genomics in snakes: differentiation, evolutionary strata, and lack of global dosage compensation. PLoS Biol. 11: 1–15.
Whitlock, M. C., and K. E. Lotterhos, 2015 Reliable detection of loci responsible for local adaptation: inference of a null model through trimming the distribution of FST. Am. Nat. 186: S24–S36.
Zeng, K., and P. Corcoran, 2015 The effects of background and interference selection on patterns of genetic variation in subdivided populations. Genetics 201: 1539–1554.

Communicating editor: W. Stephan

Appendix A: Analysis of the Two-Population Model

Following Moran (1959, 1962) (see Charlesworth and Charlesworth 2010, pp. 146–147), we assume that that migration and selection parameters are small, and we can thus approximate allele frequency changes across a generation as linear functions of migration and selection parameters (this ignores terms involving the square of migration or selection, and terms involving the product of migration and selection). Given the weak-selection assumption, allele frequencies within each deme will be approximately equal between the sexes (*e.g.*, Charlesworth and Charlesworth 2010, p. 97). The change in frequency across a single generation is:

$$\Delta q_1 = \Delta {q_1}^{\text{mig}} + \Delta {q_1}^{\text{sel}}$$

in population 1, and

$$\Delta q_2 = \Delta {q_2}^{\text{mig}} + \Delta {q_2}^{\text{sel}}$$

in population 2, where terms of $\Delta {q_j}^{\text{mig}}$ and $\Delta {q_j}^{\text{sel}}$ depend on the mode of inheritance.

Under autosomal inheritance, allele frequency changes due to migration are:

$$\Delta {q_1}^{\text{mig}} = \frac{(m_{\text{m}} + m_{\text{f}})(q_2 - q_1)}{2}$$

and

$$\Delta {q_2}^{\text{mig}} = -\frac{(m_{\text{m}} + m_{\text{f}})(q_2 - q_1)}{2}.$$

The changes due to selection are:

$$\Delta {q_1}^{\text{sel}} \approx -\frac{(s_{\text{m}} + s_{\text{f}})q_1(1 - q_1)\Big[h_1 + q_1(1 - 2h_1)\Big]}{2}$$

and

$$\Delta {q_2}^{\text{sel}} \approx \frac{(s_{\text{m}} + s_{\text{f}})q_2(1 - q_2)\Big[1 - h_2 - q_2(1 - 2h_2)\Big]}{2}.$$

At equilibrium, changes due to migration and selection balance out, leading to the set of expressions:

$$(m_{\text{m}} + m_{\text{f}})(\hat{q}_2 - \hat{q}_1) = (s_{\text{m}} + s_{\text{f}})\hat{q}_1(1 - \hat{q}_1)\Big[h_1 + \hat{q}_1(1 - 2h_1)\Big],$$

$$(s_{\text{m}} + s_{\text{f}})\hat{q}_2(1 - \hat{q}_2)\Big[1 - h_2 - \hat{q}_2(1 - 2h_2)\Big] = (m_{\text{m}} + m_{\text{m}})(\hat{q}_2 - \hat{q}_1).$$

For the case of additive effects ($h_1 = h_2 = 1/2$), these reduce to quadratic equations that can be solved as in Equation 5a.

Under *X*-linked inheritance, allele frequency changes due to migration are described by:

$$\Delta {q_1}^{\text{mig}} = \frac{2m_{\text{f}} + m_{\text{m}}}{3}(q_2 - q_1)$$

and

$$\Delta {q_2}^{\text{mig}} = -\frac{2m_{\text{f}} + m_{\text{m}}}{3}(q_2 - q_1).$$

The changes due to selection are:

$$\Delta q_1^{\text{sel}} \approx -\frac{2s_f q_1(1-q_1)\left[h_1 + q_1(1-2h_1)\right] + s_m q_1(1-q_1)}{3}$$

and

$$\Delta q_2^{\text{sel}} \approx \frac{2s_f q_2(1-q_2)\left[1-h_2 - q_2(1-2h_2)\right] + s_m q_2(1-q_2)}{3}.$$

At equilibrium, we get the following set of expressions:

$$(\hat{q}_2 - \hat{q}_1)(2m_f + m_m) = 2s_f \hat{q}_1(1-\hat{q}_1)\left[h_1 + \hat{q}_1(1-2h_1)\right] + s_m \hat{q}_1(1-\hat{q}_1),$$

$$2s_f \hat{q}_2(1-\hat{q}_2)\left[1-h_2 - \hat{q}_2(1-2h_2)\right] + s_m \hat{q}_2(1-\hat{q}_2) = (\hat{q}_2 - \hat{q}_1)(2m_f + m_m),$$

which in the additive case ($h_1 = h_2 = 1/2$) are solvable as in Equation 5b.

In cases where there is dominance, we used the equilibrium expressions above to obtain approximations for F_{ST} under conditions of high migration relative to selection. We specifically define $\delta = q_2 - q_1$ and $q = (q_1 + q_2)/2$, approximate the equilibrium expressions to first order in d in the vicinity of $\delta = 0$ (δ must be small under high migration relative to selection), and then solve for equilibrium values of q and d. These lead to the results presented in Equations 6 and 7.

Appendix B: Analysis of the Cline Models

Maximum Cline Slope

In calculating the maximum cline slope, we took the approach laid out in chapter 4 of Felsenstein (2015). As an example of the approach, consider the equilibrium for an autosomal locus in the dominance reversal model. The equilibrium reaction-diffusion equation at $x \geq 0$ is:

$$\frac{d^2q}{dx^2} = -\frac{(s_m + s_f)}{m} q(1-q)[1-h-q(1-2h)],$$

which can be rewritten in terms of the slope of the cline ($y = dq/dx$):

$$\frac{dy}{dx} = -\frac{(s_m + s_f)}{m} q(1-q)[1-h-q(1-2h)].$$

Multiplying both sides by $y = dq/dx$ leads to:

$$ydy = -\frac{(s_m + s_f)}{m} q(1-q)[1-h-q(1-2h)]dq.$$

Integrating both sides yields:

$$\frac{y^2}{2} + C = \frac{(s_m + s_f)}{12m} q^2\left[6h(1-q)^2 - q(3q-8) - 6\right],$$

where C is a constant of integration. Since $y = 0$ at $q = 1$, then $C = -(s_f + s_m)/(12m)$. The slope as a function of q, s_m, s_f, and m becomes:

$$y = \sqrt{\frac{(s_m + s_f)}{6m}\left(1 + 6hq^2(1-q)^2 - q^3(3q-8) - 6q^2\right)}.$$

The slope of the cline is steepest at the center of the range, and since the dominance reversal scenario is symmetrical around $x = 0$, $q(x = 0) = 0.5$. Therefore, the maximum slope for the autosomes becomes:

$$y = \sqrt{\frac{(s_m + s_f)(6h + 5)}{96m}},$$

which corresponds to Equation 2 from the main text [*i.e.*, after substituting $m = (m_f + m_m)/2$].

The model is slightly more complex under parallel dominance, since selection and patterns of allele frequency change are no longer symmetrical around $x = 0$. Using the same approach as above to estimating the cline slope, we obtain the following expression by analyzing the equilibrium reaction-diffusion equation for the ranges $x > 0$ and $x < 0$, respectively:

$$y^2 = \frac{(s_m + s_f)}{6m}\left\{1 - q^2\left[6 - 6h(1-q)^2 + q(3q-8)\right]\right\} \tag{B1}$$

and

$$y^2 = \frac{(s_m + s_f)}{6m}\, q^2\left[6 - 6h(1-q)^2 + q(3q-8)\right]. \tag{B2}$$

These expressions should be equal at the midpoint of the range, at which point the equilibrium frequency is the value of q that satisfies:

$$f(q) = 1 - 2q^2\left[6 - 6h(1-q)^2 + q(3q-8)\right] = 0. \tag{B3}$$

We can approximate the root by expanding $f(q)$ to second order in q around $q = 0.5$. This leads to

$$f(q) = 1 - 2q^2\left[6 - 6h(1-q)^2 + q(3q-8)\right] = 0 \approx -\frac{3}{8}(1-2h) + \frac{3}{2}(1-2q) + O\left[(q-0.5)^2\right],$$

so that the equilibrium allele frequency at the center of the range is approximately $q(x = 0) \approx (3 + 2h)/8$. This approximation matches reasonably well with the exact, numerical evaluation of the root across the full range of dominance ($0 < h < 1$), and improves as $h \to 1/2$.

We can similarly approximate the cline slope to first order in q near 0.5, which gives:

$$y^2 = \frac{(s_m + s_f)}{6m}\left(\frac{17 + 6h - 24q}{16}\right) + O\left[(q-0.5)^2\right].$$

Finally, by substituting in $q(x = 0) \approx (3 + 2h)/8$ and taking the square root, we get:

$$y \approx \frac{1}{2}\sqrt{\frac{s_m + s_f}{3m}} = \sqrt{\frac{s_m + s_f}{6(m_f + m_m)}},$$

which is presented in the main text. We confirmed by numerically evaluating Equations B1–B3 that this final result (though arrived at by approximation) actually applies generally across the full range of h. The same approach was taken to obtain X-linked clines.

Conversion of Cline Slopes to F_{ST} Metrics

To translate allele frequency cline slopes to F_{ST} values, we focus on subpopulations close to, and equidistant from, the environmental transition. (Recall that the transition occurs at location $x = 0$.) The results below apply for the additive model ($h = 1/2$). In this case, the average allele frequency for a pair of populations at opposite sides of the transition point will be $q = 1/2$.

We consider differentiation between populations slightly above and slightly below the environmental transition. For the autosomal model, the allele frequency near the cline midpoint ($x \to 0$) is approximated by

$$q_A(x) \approx \frac{1}{2} + x\sqrt{\frac{s_\mathrm{m} + s_\mathrm{f}}{6(m_\mathrm{f} + m_\mathrm{m})}},$$

which applies for subpopulations that are sufficiently close to the transition point that the allele frequency function is approximately linear. For the X chromosome, and using the same assumptions, we have:

$$q_X(x) \approx \frac{1}{2} + x\sqrt{\frac{s_\mathrm{f} + s_\mathrm{m}}{3(2m_\mathrm{f} + m_\mathrm{m})}}.$$

The autosomal and X-linked F_{ST} values between subpopulations at positions x and $-x$ are

$$F_{ST}{}^{A} = [q_A(x) - q_A(-x)]^2 \approx (2x)^2 \frac{s_\mathrm{m} + s_\mathrm{f}}{6(m_\mathrm{f} + m_\mathrm{m})}$$

and

$$F_{ST}{}^{X} = [q_X(x) - q_X(-x)]^2 \approx (2x)^2 \frac{s_\mathrm{f} + s_\mathrm{m}}{3(2m_\mathrm{f} + m_\mathrm{m})},$$

as in the main text.

Appendix C: Fitness Load of Migrant *vs.* Native Individuals in a Focal Environment

Two-Population Models

We calculate the fitness load of migrants relative to native individuals as a function of the difference in mean fitness between a migrant from one subpopulation to the other subpopulation (*e.g.*, from subpopulation 2 to 1), and the mean fitness of a native individual from the focal subpopulation (*e.g.*, from subpopulation 1). The following results apply for the additive case ($h = 1/2$). The load in the jth sex with respect to an autosomal locus is\

$$L_A = \frac{\bar{w}_{jA}(\mathrm{native}|1) - \bar{w}_{jA}(\mathrm{migrant}|2)}{\bar{w}_{jA}(\mathrm{native}|1)} \approx (\hat{q}_{2A} - \hat{q}_{1A})s_j = (1 - 2\hat{q}_{1A})s_j,$$

where overbars refer to mean fitness, the "A" subscript refers to autosomal inheritance, and terms "1" and "2" refer to subpopulation. The load for an X-linked locus is:

$$L_X = \frac{\bar{w}_{jX}(\mathrm{native}|1) - \bar{w}_{jX}(\mathrm{migrant}|2)}{\bar{w}_{jX}(\mathrm{native}|1)} \approx (\hat{q}_{2X} - \hat{q}_{1X})s_j = (1 - 2\hat{q}_{1X})s_j.$$

Assuming that s_j is the for the X and autosomes, then the relative contributions of X-linked and autosomal loci to fitness discrepancies between migrants and natives will be $L_X/L_A = \sqrt{{F_{ST}}^X/{F_{ST}}^A}$.

Cline Models

To quantify the mean fitness of migrant relative to native individuals in the cline context, we focus migrants from just above the environmental transition to just below it. The following results apply for the additive case ($h = 1/2$). Using the same approach as in Appendix B, the autosomal allele frequency near the cline midpoint ($x \to 0$) is approximated by:

$$q_A(x) \approx \frac{1}{2} + x\sqrt{\frac{s_\mathrm{m} + s_\mathrm{f}}{6(m_\mathrm{f} + m_\mathrm{m})}}.$$

The cline for the X chromosome is approximated by:

$$q_X(x) \approx \frac{1}{2} + x\sqrt{\frac{s_\mathrm{f} + s_\mathrm{m}}{3(2m_\mathrm{f} + m_\mathrm{m})}}.$$

The difference in mean relative fitness between a migrant from slightly above the environmental transition (from location x; $x > 0$) to just below it (location $-x$) and a native individual from location $-x$ is

$$L_A = \lim_{x\to 0} \frac{\bar{w}_{jA}(\text{native}|-x) - \bar{w}_{jA}(\text{migrant}|x)}{\bar{w}_{jA}(\text{native}|-x)} = 2xs_j\sqrt{\frac{s_\mathrm{m} + s_\mathrm{f}}{6(m_\mathrm{f} + m_\mathrm{m})}}$$

and

$$L_X = \lim_{x\to 0} \frac{\bar{w}_{jX}(\text{native}|-x) - \bar{w}_{jX}(\text{migrant}|x)}{\bar{w}_{jX}(\text{native}|-x)} = 2xs_j\sqrt{\frac{s_\mathrm{f} + s_\mathrm{m}}{3(2m_\mathrm{f} + m_\mathrm{m})}}.$$

Therefore, the relative contributions of X-linked and autosomal loci to fitness discrepancies between migrants and natives is $L_X/L_A = y_X/y_A$.